Phase-dependent electromagnetically induced transparency and its dispersion properties in a four-level quantum well system

Amitabh Joshi*
Department of Physics, University of Arkansas, Fayetteville, Arkansas 72701, USA
and Department of Physics, Eastern Illinois University, Charleston, Illinois 61920, USA
(Received 20 May 2008; published 24 March 2009)

The four-level inverted-Y configuration realizable in an asymmetric quantum well system interacting with four fields is studied to demonstrate the phenomenon of phase-dependent electromagnetically induced transparency (EIT) in this system. The system is studied under various parametric conditions to demonstrate the controllability of EIT, dispersion properties, and group velocity.

DOI: 10.1103/PhysRevB.79.115315 PACS number(s): 78.67.De, 42.50.Hz, 42.50.Gy

I. INTRODUCTION

During the last decade the phenomenon of electromagnetically induced transparency (EIT) (Refs. 1 and 2) in three-level systems has been a center of attraction. Basically this phenomenon describes inhibition of absorption in a three-level medium to a resonant probe-laser field due to the application of a strong-coupling laser field to other transitions. Numerous applications of EIT have been proposed that include lasing without population inversion,[3] enhanced nonlinear optical processes,[4] to quantum computation and communications.[5] In the recent past, EIT in four-level atomic systems under different configurations with some experimental realization has also been reported.[6,7]

Many important phenomena of atomic-molecular three-level systems have been extended to their semiconductor counterparts, e.g., quantum optical coherence and interference effects[4] have been studied in intersubband transitions in the conduction band of semiconductor quantum wells (QWs). Some of these phenomena studied in semiconductor QWs are electromagnetically induced transparency (EIT),[8] enhanced nonlinear processes,[9] lasing without inversion (LWI),[10] and optical Stark effect.[11] Observation of coherent phenomena in these systems is limited because of the large dephasing rates in semiconductors (~ 10 ps^{-1}). The advantages of using QWs are that their transition energies, dipole moments, and symmetries can be engineered as desired and the dipole moments of intersubband transitions are large. Some Fano interference schemes have been used to demonstrate the viability of quantum interference and EIT in QW systems. EIT was recently demonstrated in an n-doped InGaAs QW (with an AlInAs barrier) which could be described as a three-level ladder-type system.[8] A strong driving field, which is in two-photon resonance with the system and simultaneously drives all three states into coherence, results in a "locking" of quantum phases.[8] This system gives rise to an enhanced transparency feature in the absorption spectrum. The optical bistability in such a system under similar experimental conditions was studied and the controlled performances of this bistable device with different parameters were demonstrated.[12] Further to this, the coherent control of optical processes in atomic, molecular, and condensed-matter systems has been achieved by changing the relative phase of applied laser fields.[13] In the atomic configuration with closed-loop interaction scheme, the relative phase of fields becomes very important. It can modify linear and nonlinear properties dramatically and can give rise to several interesting phenomena. The closed-loop interaction schemes could be used for phase-controlled EIT,[14] coherent population transfer,[15] manipulation of spontaneous emission spectra, etc.[16] Phase control of electron population, absorption, and dispersion properties of the semiconductor quantum well was also studied. The quantum well considered in that study was an asymmetric quantum well having a three-level cascade configuration interacting with a laser field and its second harmonic.[17] In another interesting work tunneling-induced transparency in an asymmetric double quantum well structure was studied where Fano-type interferences for the collective intersubband excitation were observed.[18] Inspired by these studies we study the phase-controlled EIT, dispersive properties, and group-velocity reduction in an asymmetric double quantum well system consisting of four energy levels in an inverted-Y configuration interacting with different laser fields. This is because the phase-dependent effects have inherent tunability associated with them with an easily controllable single parameter. The transitions depicted in Fig. 1 are all dipole allowed. By analytical and numerical calculations,

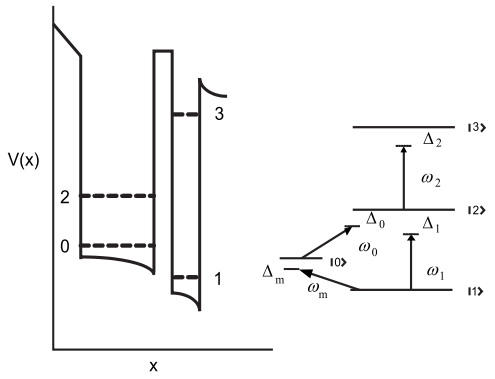

FIG. 1. (a) Schematic band diagram of a single period of the asymmetric double quantum well system with potential $V(x)$ as a function of x, having four discrete levels. (b) Schematic energy-level diagram of a four-level system in inverted-Y configuration for (a). Here, ω_1 (Δ_1), ω_0 (Δ_0), ω_2 (Δ_2), and ω_m (Δ_m) are frequencies (frequency detunings) of probe, coupling, pumping, and cycling fields, respectively.

we find few interesting properties due to the effect of the closed interaction phase. We find that not only the strengths of applied laser fields but also the total closed interaction phase can modify the position, the shape, and the widths of the EIT structure. Also, corresponding to the specific phase, the strengths and the frequency detunings of applied laser fields behave differently on the frequency intervals of double EIT. The system of inverted-Y configuration can be easily realized in intersubband transitions in the conduction band of semiconductor quantum wells. The two-dimensional electron gas behaves effectively as a single oscillator due to strong electron-electron interaction and thus the system gives rise to atomlike absorption-dispersion behavior. The advantage of the quantum well system over the atomic system is that the intersubband energies and the electron wave function symmetries can be engineered as desired in accordance with the requirements.

The system of four levels in inverted-Y configuration gives rise to double-dark resonances and double EIT with two control fields which are not available in the three-level systems. We will see in the following that the frequency detunings of these control fields are very much crucial to determine the shape and width of double-EIT features and hence advantageous over any three-level system because of this flexibility. Note that the double-dark resonances play an important role in unipolar and bipolar quantum well lasers and there is a potential application of double-dark states in adiabatic passage techniques.

In the recent past there has been an upsurge in the study of group velocity using EIT exhibiting atomic media in subluminal and superluminal regimes to realize single-photon switching by quantum interference, to search for quasitachyons, to create atomic dielectric analogs of gravitational field, etc. The EIT media exhibit steep linear and nonlinear dispersions and show reduction of group velocity in thermal atomic vapor, Bose-Einstein condensate, ruby crystal at room temperature, and solid hydrogen. The quantum well could be a more practical device for such purposes and we study the group-velocity behavior for such devices in this study. In view of many potential applications of ultraslow and superluminal light propagation, a question of interest is whether one can have a controlling parameter in a single experiment for switching from subluminal to superluminal propagation. In this paper we propose a scheme based on four-level EIT in which we can switch the propagation of light from subluminal to superluminal by changing the phase of one of the driving fields. It is the phase of this driving field that affects the medium dispersion in such a way that we can have a switching from subluminal to superluminal group velocity. We will demonstrate the control of group velocity using the phase parameter such that continuous tuning of group velocity could be possible from subluminal to superluminal and vice versa.

The rest of the paper is organized as follows. In Sec. II, we present our model and its approximate solution. In Sec. III, we present exact numerical results and their discussion. This is followed by concluding remarks in Sec. IV.

II. MODEL

In this work, we consider a closed four-level inverted-Y configuration in an asymmetric quantum well system as shown in Fig. 1, which has been realized experimentally. Levels $|1\rangle$, $|2\rangle$, and $|3\rangle$ are in a usual three-level ladder-type configuration and level $|0\rangle$ together with levels $|1\rangle$ and $|2\rangle$ forms a three-level Λ-type configuration. So, this composite system consists of two subsystems, i.e., one ladder type and the other Λ type. The description of the optically allowed transitions in this system is as follows. The transition $|1\rangle$ to $|2\rangle$ (transition frequency ω_{12}) interacts with a weak probe field E_1 (frequency ω_1) having Rabi frequency $2\Omega_1 = E_1 d_{12}/\hbar$. A coupling field E_0 (frequency ω_0) drives the transition $|0\rangle$ to $|2\rangle$ (with transition frequency ω_{02}) with a Rabi frequency of $2\Omega_0 = E_0 d_{02}/\hbar$ while a pumping field E_2 (frequency ω_2) is acting on transitions $|2\rangle$ and $|3\rangle$ (with transition frequency ω_{23}) and has a Rabi frequency equal to $2\Omega_2 = E_2 d_{23}/\hbar$. A cycling field (frequency ω_m) is coupled to the transition $|1\rangle$ to $|0\rangle$ (with transition frequency ω_{01}) and has a Rabi frequency equal to $2\Omega_m = E_m d_{01}/\hbar$. The decay constants from levels $|3\rangle$ to $|2\rangle$, $|2\rangle$ to $|0\rangle$, $|0\rangle$ to $|1\rangle$, and $|2\rangle$ to $|1\rangle$ are γ_3, γ_2, γ_0, and γ_1, respectively. The decay constants in semiconductor quantum wells are comprised of a population-decay contribution as well as a dephasing contribution. The first contribution is mainly due to longitudinal optical (LO) photon emission at low temperature and the other contribution comes from electron-phonon scattering and scattering on interface roughness.[19] For a typical double quantum well structure[20] it is possible to realize the following values for the decay constants: $2\gamma_1 = 2\gamma_1 = 2\gamma_3 = 4-6$ meV, $2\gamma_0 = 0.2$ meV. The corresponding atomic detunings for these transitions are $\Delta_2 = \omega_2 - \omega_{23}$, $\Delta_0 = \omega_0 - \omega_{02}$, $\Delta_m = \omega_m - \omega_{10}$, and $\Delta_1 = \omega_1 - \omega_{12}$, respectively. In this way, two middle levels $|0\rangle$ and $|2\rangle$, upper level $|3\rangle$, and the ground level $|1\rangle$ form a closed interaction contour. The phases associated with the four coherent fields Ω_0, Ω_1, Ω_2, and Ω_m are ϕ_0, ϕ_1, ϕ_2, and ϕ_m, respectively.

If there is no coupling field and E_m is zero then this configuration reduces to a standard ladder-type three-level EIT system driven by the probe and the pumping fields. On the other hand if we set the pumping field E_2 along with E_m to zero then this configuration along with probe and coupling fields forms a standard Λ-type three-level EIT system. The system can be easily realized experimentally with carbon dioxide laser frequencies, which can be derived from the same parent laser and can be frequency tuned with acousto-optic modulators or gratings. Thus the fundamental frequency of this laser can be tuned in such a way to excite all the three transitions mentioned above in an asymmetric quantum well maintaining a relative phase control of all the fields. The small signal absorption of the weak-probe field propagating through such a system can be computed in the steady state. The density-matrix equations of motion in dipole and rotating-wave approximations for this system can be written as follows:

$$\dot{\rho}_{11} = 2\gamma_1\rho_{22} + 2\gamma_0\rho_{00} + i\Omega_1(\rho_{12} - \rho_{21}) + i\Omega_m(\rho_{10} - \rho_{01}),$$

$$\dot{\rho}_{22} = -2(\gamma_1 + \gamma_2)\rho_{22} + 2\gamma_3\rho_{33} - i\Omega_1(\rho_{12} - \rho_{21}) - i\Omega_0(\rho_{02} - \rho_{20}) + i\Omega_2(\rho_{23} - \rho_{32}),$$

$$\dot{\rho}_{33} = -2\gamma_3\rho_{33} - i\Omega_2(\rho_{23} - \rho_{32}),$$

$$\dot{\rho}_{00} = 2\gamma_2\rho_{22} - 2\gamma_0\rho_{00} + i\Omega_0(\rho_{02} - \rho_{20}) - i\Omega_m(\rho_{10} - \rho_{01}),$$

$$\dot{\rho}_{12} = -(\gamma_1 + \gamma_2 - i\Delta_1)\rho_{12} + i\Omega_0\rho_{10}e^{i\Phi} + i\Omega_2\rho_{13} + i\Omega_1(\rho_{11} - \rho_{22}) - i\Omega_m\rho_{02}e^{i\Phi},$$

$$\dot{\rho}_{13} = -[\gamma_3 - i(\Delta_1 + \Delta_2)]\rho_{13} + i\Omega_2\rho_{12} - i\Omega_1\rho_{23} - i\Omega_m\rho_{03},$$

$$\dot{\rho}_{23} = -(\gamma_1 + \gamma_2 + \gamma_3 - i\Delta_2)\rho_{23} - i\Omega_1\rho_{13} - i\Omega_0\rho_{03}e^{-i\Phi} + i\Omega_2(\rho_{22} - \rho_{33}),$$

$$\dot{\rho}_{10} = -[\gamma_0 - i(\Delta_1 - \Delta_0 - \Delta_m)]\rho_{10} + i\Omega_0\rho_{12}e^{-i\Phi} - i\Omega_1\rho_{20}e^{-i\Phi} - i\Omega_m(\rho_{00} - \rho_{11}),$$

$$\dot{\rho}_{02} = -[\gamma_1 + \gamma_2 - i(\Delta_0 + \Delta_m)]\rho_{02} + i\Omega_1\rho_{01}e^{-i\Phi} + i\Omega_2\rho_{03}e^{-i\Phi} + i\Omega_0(\rho_{00} - \rho_{22}) - i\Omega_m\rho_{12}e^{-i\Phi},$$

$$\dot{\rho}_{03} = -[\gamma_0 + \gamma_3 - i(\Delta_0 + \Delta_m + \Delta_2)]\rho_{03} + i\Omega_2\rho_{02}e^{i\Phi} - i\Omega_0\rho_{23}e^{i\Phi} - i\Omega_m\rho_{13}, \quad (1)$$

in which $\Phi = \phi_2 + \phi_m - \phi_0$ and the trace condition $\Sigma_i \rho_{ii} = 1$. For obtaining linear susceptibility, we need to solve the density matrix equations (1) under the steady-state condition. Under the assumption that the coupling field (E_0) and the pumping field (E_2) are much stronger than the probe field (E_1), it can be assumed that almost all the atoms are in the ground state $|1\rangle$. Under the weak-probe field approximation, the expression of the ρ_{12}, ρ_{20} in the first order goes as

$$\rho_{21} = \left[-i\Omega_1(\rho_{11} - \rho_{22}) + \frac{\Omega_0\Omega_m e^{-i\Phi}}{\gamma_1 + i(\Delta_1 - \Delta_2)}(\rho_{00} - \rho_{11}) + \left(\frac{i\Omega_0^2\Omega_1}{\gamma_0 + i(\Delta_1 - \Delta_0)(\gamma_1 + \gamma_2 - i\Delta_0)} + \frac{\Omega_m\Omega_0 e^{-i\Phi}}{\gamma_1 + \gamma_2 + i\Delta_0} \right) \times (\rho_{00} - \rho_{22}) \right] \left[(\gamma_1 + \gamma_2 + i\Delta_1) + \frac{\Omega_0^2}{\gamma_0 + i(\Delta_1 - \Delta_0)} + \frac{\Omega_2^2}{\gamma_3 + i(\Delta_1 + \Delta_2)} + \frac{\Omega_m^2}{\gamma_1 + \gamma_2 + i\Delta_0} \right]^{-1}, \quad (2)$$

$$\rho_{20} = \left[-i\Omega_1(\rho_{00} - \rho_{22}) - \frac{\Omega_1\Omega_m}{\gamma_0 - i(\Delta_1 - \Delta_0)}(\rho_{00} - \rho_{11}) + \left(\frac{i\Omega_0\Omega_1^2}{\gamma_0 - i(\Delta_1 - \Delta_0)(\gamma_1 + \gamma_2 - i\Delta_1)} + \frac{\Omega_m\Omega_0 e^{i\Phi}}{\gamma_1 + \gamma_2 + i\Delta_1} \right) \times (\rho_{11} - \rho_{22}) \right] \left[(\gamma_1 + \gamma_2 + i\Delta_0) + \frac{\Omega_1^2}{\gamma_0 - i(\Delta_1 - \Delta_0)} + \frac{\Omega_2^2}{\gamma_0 + \gamma_3 + i(\Delta_0 + \Delta_3)} + \frac{\Omega_m^2}{\gamma_1 + \gamma_2 + i\Delta_1} \right]^{-1}. \quad (3)$$

To obtain Eqs. (2) and (3), we assumed that initially the values of ρ_{20} and ρ_{23} are approximately zero and Δ_m is absorbed in Δ_0, meaning we redefine Δ_0 ($\equiv \Delta_0 + \Delta_m$), while writing down Eqs. (2) and (3). The other ρ_{ii} ($i = 0, 1, 2$) in the right-hand sides of Eqs. (2) and (3) are of zeroth order. Equation (2) gives some ideas of how the coupling field (E_0) and the pumping field (E_2) affect the absorption and dispersion properties of the probe field E_1, which give rise to the EIT conditions. When $E_2 = E_m = 0$, we get the EIT equation [from Eq. (2)] for a three-level system in a Λ-type configuration. On the other hand when $E_0 = E_m = 0$, then Eq. (2) reduces to the EIT equation for a three-level system in a ladder-type configuration. Note that Eqs. (2) and (3) are strictly valid only under the weak-probe field approximation so we will concentrate on more general results using numerical solutions of Eq. (1) in the steady-state limit without invoking the weak-probe field approximation.

One can calculate the group velocity v_g of the probe field by using the expression

$$v_g/c = \frac{1}{\left[1 + 2\pi\,\mathrm{Re}(\chi) + 2\pi\omega_1 \frac{\partial\,\mathrm{Re}(\chi)}{\partial\omega_1} \right]}, \quad (4)$$

where we have defined the probe susceptibility $\chi = \rho_{12}/\Omega_1$. The other quantity relevant for this purpose is the group index $n_g = c/v_g - 1$,

$$c/v_g - 1 = 2\pi\,\mathrm{Re}(\chi) + 2\pi\omega_1 \frac{\partial\,\mathrm{Re}(\chi)}{\partial\omega_1}. \quad (5)$$

The dependence of group velocity comes through the real part of the susceptibility which is related to the imaginary part by Kramers-Kronig relations and hence we need to find carefully both the quantities and thus the conditions for phase control of group velocity.

III. NUMERICAL RESULTS AND DISCUSSION

Now we elaborate the results for this composite EIT system by numerical integration of Eq. (1) in the steady-state condition. For this purpose we will examine the coherence term ρ_{12} for the probe transition in terms of its real and imaginary parts as a function of probe field frequency detuning Δ_1/γ_1. The imaginary and the real parts of ρ_{12} versus Δ_1/γ_1 represent the probe field absorption and dispersion spectra, respectively, up to all orders. The numerical results match well with the approximate results [Eq. (2)] under the appropriate conditions of parameters.

The asymmetric quantum well sample for the current study can be very much similar to the one used in Refs. 8, 17, and 18 so that we can keep the same parametric conditions here. These quantum well samples are grown by the molecular-beam epitaxy (MBE) method with 40–80 symmetric 10 nm n-doped ($n_s = 6 \times 10^{11}$ cm^{-2}) $In_xGa_{1-x}As$ ($x = 0.47$) wells and 10 nm $Al_yIn_{1-y}As$ ($y = 0.48$) barriers supported on a lattice-matched undoped InP substrate containing a 1–2 mm diameter etched hole for optical access. The sample can be designed to have desired transition energies in the range of 120–170 meV and desired dipole moments. Alternatively, an asymmetric quantum well structure may be consisting of 40–60 modulation-doped coupled quantum wells. These GaAs quantum wells (with approximate thicknesses of 6–8 nm) separated by an $Al_{0.33}Ga_{0.67}As$ barrier (2

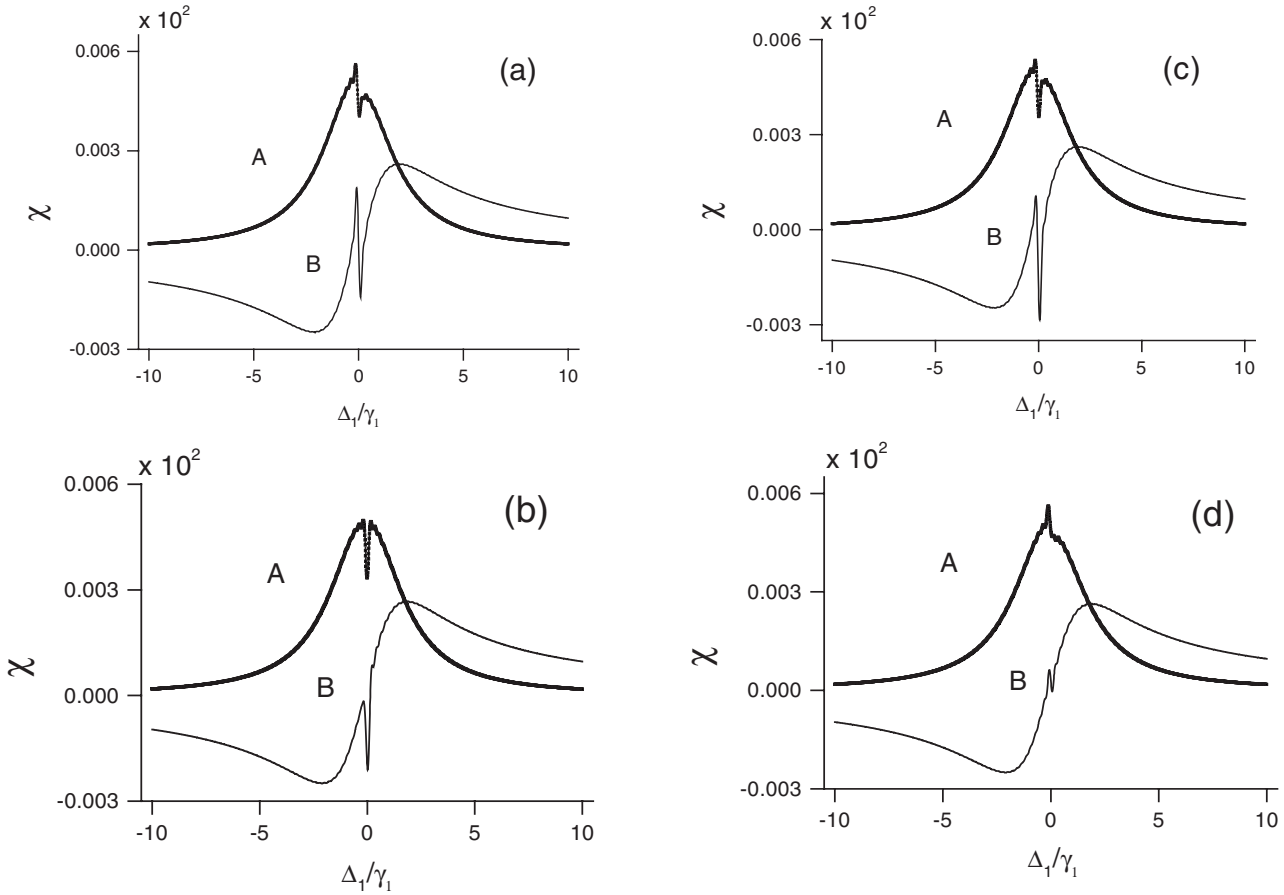

FIG. 2. Imaginary and real parts of the susceptibility (χ) represented by curves A and B, respectively, as a function of Δ_1/γ_1 for the parametric conditions $\gamma_1=\gamma_2=\gamma_3=1.0$, $\Delta_0/\gamma_1=\Delta_2/\gamma_1=0.0$, $\Omega_1/\gamma_1=0.01$, $\Omega_0/\gamma_1=0.5$, $\Omega_2/\gamma_1=0.2$, and $\Omega_m/\gamma_1=0.5$. Here plots (a), (b), (c) and (d) are for $\Phi=0$, $\Phi=\pi/2$, $\Phi=\pi/4$, and $\Phi=-\pi/4$, respectively.

nm thickness) can be grown on the GaAs substrate.[20] The coupled well periods can have separation of 95 nm by inserting another spacer of $Al_{0.33}Ga_{0.67}As$. This structure could be designed to meet the transition energy requirements of 120–180 meV and desired dipole moments, which can easily be accessible with an available semiconductor diode laser system in the midinfrared range. In fact, one can use continuous-wave tunable cryogenic lead-salt diode lasers made from IV-VI semiconductor materials, carbon dioxide lasers, or quantum cascade lasers, e.g., independently tunable lasers with similar temporal profiles (say several hundreds of picoseconds) in $Er^{3+}:Cr^{3+}:YSGG$-laser pumped optical parametric generators (OPOs) based on $ZnGeP_2$ and CdSe nonlinear crystals. All these lasers/OPOs have narrow linewidths compared to the intersubband dephasing rate. The peak intensities are up to the orders of 2.6 MW/cm^2 and controllable with external means. The lasers/OPOs can be controlled by a master oscillator or triggering system to maintain a phase difference among them. The photon drag with amplifier (PDA) detector or any fast detector with reasonable sensitivity would be suitable for the experiment.

We first concentrate on the situation when EIT is controlled by a single parameter Φ (in Fig. 2) under the condition of atoms initially (at $t=0$) in state ($|1\rangle$), with $\Delta_0/\gamma_1=\Delta_2/\gamma_1=\Delta_m/\gamma_1=0$ and other parameters are $\gamma_2/\gamma_1=\gamma_3/\gamma_1=1.0$ (typically $2\gamma_1=5$ meV in the realistic quantum well system, and we set this value for γ_1 for all the results presented here in this work), $\gamma_0/\gamma_1=0.04$, $\Omega_1/\gamma_1=0.005$, $\Omega_0/\gamma_1=0.5$, $\Omega_2/\gamma_1=0.2$, and $\Omega_m/\gamma_1=0.5$. In Fig. 2 plots of Im (ρ_{12}) (curve A) and Re (ρ_{12}) (curve B) as a function of Δ_1/γ_1 are shown. Plots (a), (b), (c), and (d) are for $\Phi=0$, $\Phi=\pi/2$, $\Phi=\pi/4$, and $\Phi=-\pi/4$, respectively. In all these curves we see the combined effect of two subsystems (the Λ-type subsystem and the ladder-type subsystem) along with the effect of field Ω_m. Thus each curve marked as A has a double-EIT feature and curve B has a dispersion feature corresponding to the double EIT. This means that in the steady-state limit, both coherences ρ_{01} and ρ_{31} get developed which is reflected in the probe absorption spectrum in terms of double EIT. The system exhibits both absorption and dispersion controls with the single phase parameter Φ. At the two-photon resonant condition there is a merger of two dips. This system can be analyzed in terms of the dressed states created by the coupling field and the pumping field. It is the destructive interference between two excitation pathways to these dressed states from the ground state $|1\rangle$ that gives rise to the EIT. We can see this by taking one sample as an example. In the resonant condition, the interaction Hamiltonian (for $\Phi=0$) is $H=\hbar\Omega_1|1\rangle\langle 2|+\hbar\Omega_0|0\rangle\langle 2|+\hbar\Omega_m|0\rangle\langle 1|+\hbar\Omega_2|2\rangle\langle 3|$ +H.c., where $|1\rangle$, $|0\rangle$, $|2\rangle$, and $|3\rangle$ are the discrete states (Fig. 1). The approximate eigenvalues of this Hamiltonian are 0, 0, $\pm\sqrt{\Omega_1^2+\Omega_0^2+\Omega_m^2+\Omega_2^2}$, respectively, for the selected

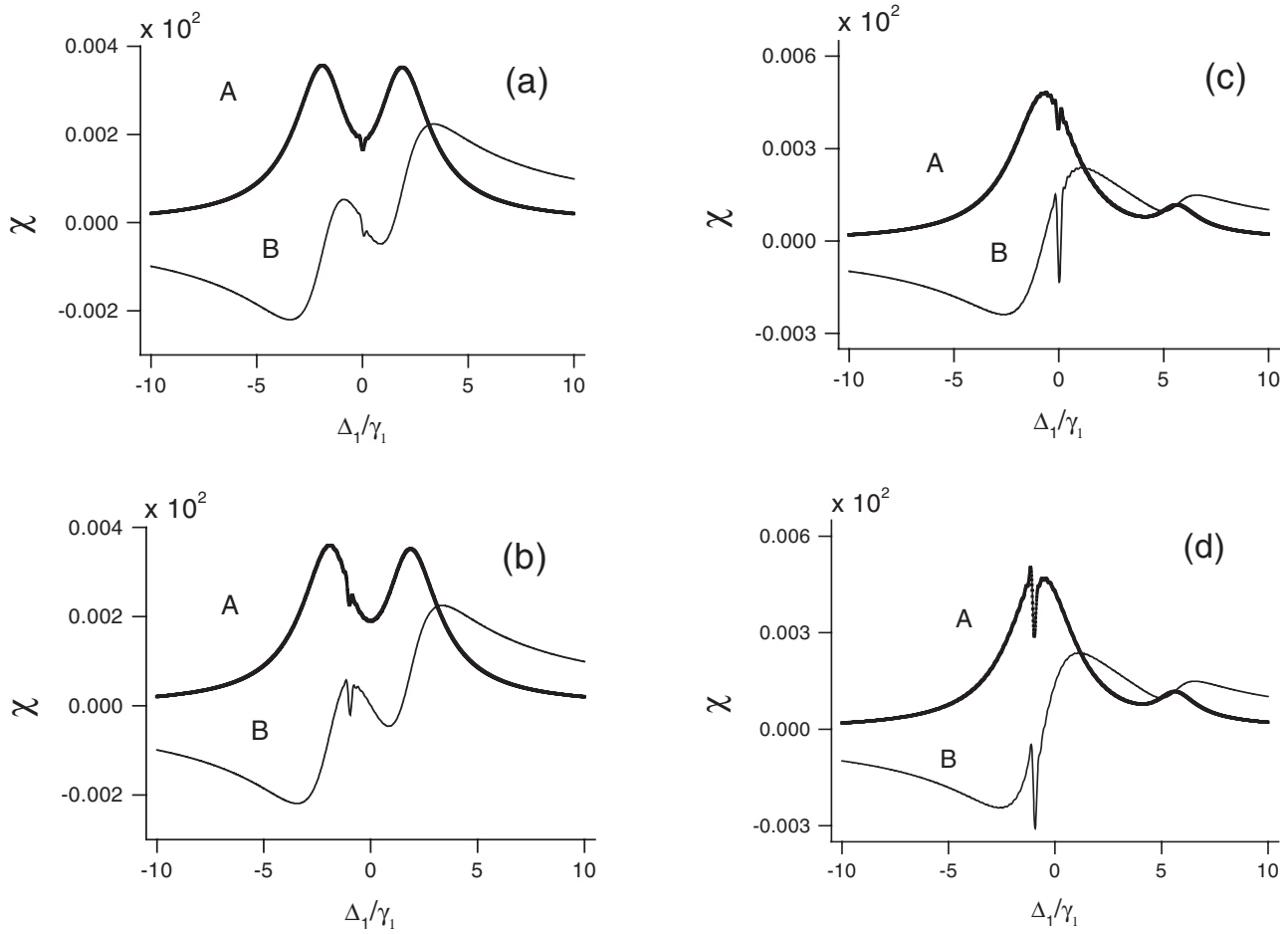

FIG. 3. Imaginary and real parts of the susceptibility (χ) represented by curves A and B, respectively, as a function of Δ_1/γ_1 for the parametric conditions $\Phi=\pi/3$, $\Omega_1/\gamma_1=0.005$, $\Omega_0/\gamma_1=0.5$, $\Omega_2/\gamma_1=1.5$, $\Omega_m/\gamma_1=1.0$, and $\Delta_m/\gamma_1=0$. Here plots (a), (b), (c), and (d) are for $(\Delta_0/\gamma_1=0,\ \Delta_2/\gamma_1=0)$, $(\Delta_0/\gamma_1=0,\ \Delta_2/\gamma_1=-5)$, $(\Delta_0/\gamma_1=-1,\ \Delta_2/\gamma_1=0)$, and $(\Delta_0/\gamma_1=-1,\ \Delta_2/\gamma_1=-5)$, respectively.

field values. The corresponding eigenstates to the zero eigenvalues are linear combinations of the states $|1\rangle$, $|0\rangle$, and $|3\rangle$. Thus, we have two dark states or the degenerated dark states in this case. If the atoms are in any or both of the dark states then EIT is exhibited. Under the exact resonance condition, we observe overlap of double EIT as the two dark states are degenerate. Since the field strengths of coupling and pump fields are nearly the same, so the resultant EIT pattern is very much sensitive to the phase parameter. The EIT feature [$\mathrm{Im}(\rho_{12})$: curve A] and the corresponding refractive index [$\mathrm{Re}(\rho_{12})$: curve B] exhibit dispersionlike profiles when $\Phi=0$ [Fig. 2(a)] and absorptionlike profiles when $\Phi=\pi/2$ [Fig. 2(b)]. This behavior of the EIT phenomenon at the exact resonance condition of all the fields is very much different from any three-level system and thus nontrivial. For $\phi=\pi/4$, we get profiles of curves A and B [Fig. 2(c)] as intermediate to the $\phi=0$ and $\phi=\pi/2$ cases as discussed above. However, for $\phi=-\pi/4$, these profiles show negative absorption [curve A: Fig. 2(d)] and reduced central dispersion feature [curve B: Fig. 2(d)]. The interesting aspect of this EIT situation is its controllability by appropriately selecting the experimental parameters. This has been depicted in Fig. 3 where the phase parameter has been kept fixed ($\Phi=\pi/3$) along with Rabi frequencies $\Omega_1/\gamma_1=0.005$, $\Omega_0/\gamma_1=0.5$, $\Omega_2/\gamma_1=1.5$, $\Omega_m/\gamma_1=1.0$, and $\Delta_m/\gamma_1=0$. In Fig. 3 the plots (a), (b), (c), and (d) are for $(\Delta_0/\gamma_1=0,\ \Delta_2/\gamma_1=0)$, $(\Delta_0/\gamma_1=0,\ \Delta_2/\gamma_1=-5)$, $(\Delta_0/\gamma_1=-1,\ \Delta_2/\gamma_1=0)$, and $(\Delta_0/\gamma_1=-1,\ \Delta_2/\gamma_1=-5)$, respectively. We can now clearly resolve the double-EIT features in these curves because of the large difference in coupling and pumping field strengths as well as nonzero values of frequency detunings of these controlling fields. This implies that field strengths along with frequency detunings of the coupling laser and the pumping laser fields can lead to controlling of the double-EIT width, shape, and location very effectively—something difficult to achieve with one of the subsystems consisting of a three-level configuration alone. The dispersion properties represented by these curves are again the combined response of two three-level subsystems. The locations of peaks and dips are sensitive functions of the values of Δ_0/γ_1 and Δ_2/γ_1, which can be clearly observed in curve B of Fig. 3. This is because the dark states have shifted according to the selected values of Δ_0/γ_1 and Δ_2/γ_1. In Fig. 4 we have continued the exploration of EIT controllability by appropriately selecting the experimental parameters. This time the parameters are $\Omega_1/\gamma_1=0.005$, $\Omega_0/\gamma_1=0.5$, $\Omega_2/\gamma_1=1.5$, $\Omega_m/\gamma_1=1.0$, and $\Delta_m/\gamma_1=0$. The plots (a), (b), and (c) are for $(\Phi=\pi,\ \Delta_0/\gamma_1=0,\ \Delta_2/\gamma_1=0)$, $(\Phi=\pi,\ \Delta_0/\gamma_1=-1,\ \Delta_2/\gamma_1=-5)$, and $(\Phi=\pi/2,\ \Delta_0/\gamma_1=-1,\ \Delta_2/\gamma_1=-5)$, respectively. Again curves in (b) and (c) clearly show well

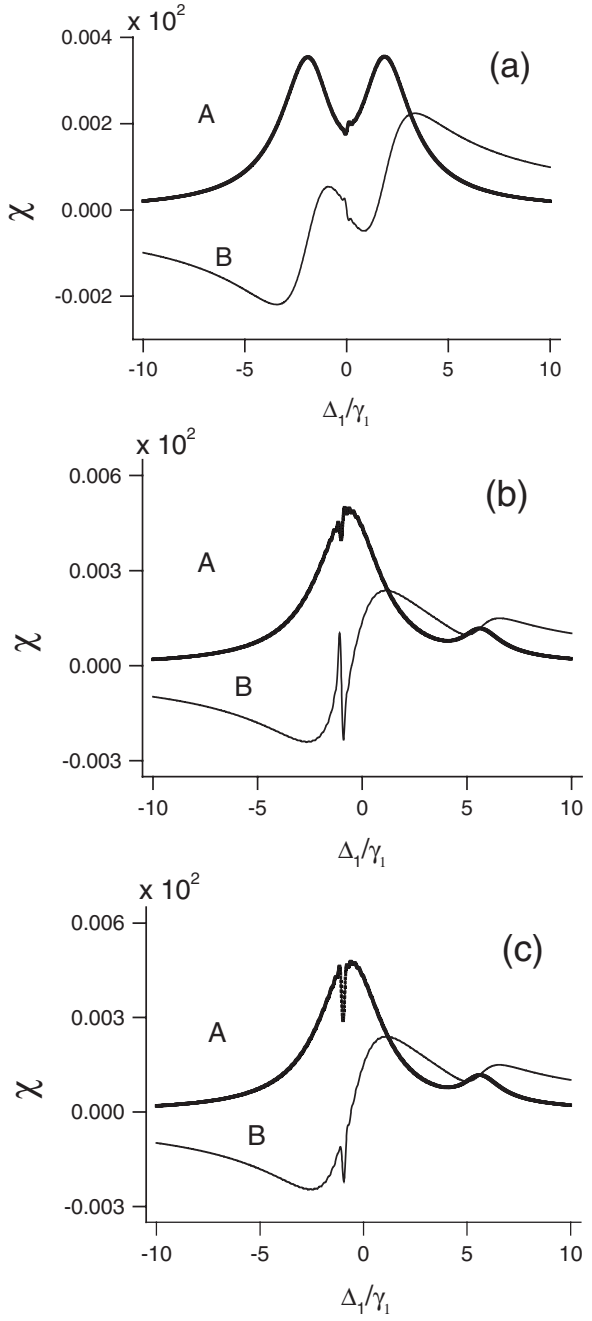

FIG. 4. Imaginary and real parts of the susceptibility (χ) represented by curves A and B, respectively, as a function of Δ_1/γ_1 for the parametric conditions $\Omega_1/\gamma_1=0.005$, $\Omega_0/\gamma_1=0.5$, $\Omega_2/\gamma_1=1.5$, $\Omega_m/\gamma_1=1.0$, and $\Delta_m/\gamma_1=0$. Here plots (a), (b), and (c) are for ($\Phi=\pi$, $\Delta_0/\gamma_1=0$, $\Delta_2/\gamma_1=0$), ($\Phi=\pi$, $\Delta_0/\gamma_1=-1$, $\Delta_2/\gamma_1=-5$), and ($\Phi=\pi/2$, $\Delta_0/\gamma_1=-1$, $\Delta_2/\gamma_1=-5$), respectively.

separated double EIT and the corresponding dispersion is clearly due to the large value of Δ_2 and Δ_0. The EIT peaks [curve A in (b) and (c)] are shifted in the opposite direction from the center point ($\Delta_1=0$) because the two subsystems have opposite responses to the same sign of respective detunings of their control field frequencies.

We further study this EIT system for the group-velocity variation with the phase factor Φ. For this purpose we plot the group index c/v_g-1 with the exact solution of Eq. (1) as a function of Δ_1/γ_1 in Figs. 5(a)–5(c) and as a function of Φ in Fig. 5(d). For all these curves we set $\Delta_0/\gamma_1=\Delta_2/\gamma_1=\Delta_m/\gamma_1=0$, $\gamma_2/\gamma_1=\gamma_3/\gamma_1=1.0$, $\gamma_0/\gamma_1=0.04$, $\Omega_1/\gamma_1=0.005$, $\Omega_0/\gamma_1=0.5$, $\Omega_2/\gamma_1=0.2$, and $\Omega_m/\gamma_1=0.5$. Figures 5(a)–5(c) are for $\Phi=0$, $\pi/3$, and $-\pi/4$, respectively. All these plots (a)–(c) are showing switching in the group velocity of the probe field from subluminal to superluminal for three different values of Φ. The interesting feature of such switch is provided in Fig. 5(b), where just by changing the sign of Δ_1/γ_1 from negative to positive from the central position gives rise to the change of group velocity from subluminal to superluminal. We have considered a modest value of frequency of the probe field: $\omega_1=1000\gamma_1$. Figure 5(d) shows (with $\Delta_1/\gamma_1=0$) variation of the group-velocity index as a function of Φ. Thus with a single parameter Φ the group velocity can be controlled as desired.

In order to estimate the total number of bits that can be stored in the four-level inverted-Y type configuration, we can write the delay bandwidth product $N_{\text{total}}=T_{\text{abs}}B_W$, which increases with the EIT bandwidth.[21] The EIT bandwidth is a crucial function of γ_0, γ_3, Ω_0, Ω_2, etc. The delay time T_{abs} is related to the group index $[n_g(0)]$ and absorption coefficient $\alpha(0)$ in the following way:

$$T_{\text{abs}}=n_g(0)\frac{ln2}{\alpha(0)c}, \tag{6}$$

where

$$\begin{aligned} n_g(0)=\bar{n}+\bar{n}\Omega_{PL}^2\times[&(1-\Omega_0\Omega_m'\sin(\Phi))(\gamma_1+\gamma_2)(\gamma_0+\gamma_3)\\ &\times[(\gamma_1+\gamma_2)^2\gamma_0\gamma_3+(\gamma_1+\gamma_2)(\Omega_0^2\gamma_3+\Omega_2^2\gamma_0)\\ &+\Omega_m^2\gamma_0\gamma_3]-(1-\Omega_0\Omega_m'\sin(\Phi))\gamma_0\gamma_3(\gamma_1+\gamma_2)^2\\ &\times[\gamma_0\gamma_3+(\gamma_0+\gamma_3)(\gamma_1+\gamma_2)\\ &+(\Omega_0^2+\Omega_2^2+\Omega_m^2(\gamma_0+\gamma_3)/(\gamma_1+\gamma_2))]]\\ &\times[(\gamma_1+\gamma_2)^2\gamma_0\gamma_3+(\gamma_1+\gamma_2)(\Omega_0^2\gamma_3+\Omega_2^2\gamma_0)\\ &+\Omega_m^2\gamma_0\gamma_3]^{-2}, \end{aligned}$$

$$\alpha(0)=\frac{2\bar{n}}{c}\Omega_{PL}^2[1-\Omega_0\Omega_m'\sin(\Phi)]\times\left[(\gamma_1+\gamma_2)+\frac{\Omega_0^2}{\gamma_0}+\frac{\Omega_2^2}{\gamma_2}+\frac{\Omega_m^2}{(\gamma_1+\gamma_2)}\right]^{-1},$$

$$\Omega_{PL}^2=\frac{Ne^2f_P}{4\bar{n}^2m_0\epsilon_0}, \tag{7}$$

at the exact resonance condition of all the fields ($\Delta_0=\Delta_1=\Delta_2=\Delta_m=0$). Here, $\bar{n}$ is the refractive index, $\Omega_m'=\Omega_m/\Omega_1$, N is the concentration of active atoms, and f_P is the oscillator strength of the probe transition.

From the above Eqs. (6) and (7), it is clear that the delay time is a sensitive function of the strengths of coupling and pumping fields and the relative phase Φ. Thus the controllability of delay time in such a four-level system has more flexibility (in terms of parametric control) compared to a three-level system. It is easy to see that at $\Phi=0$ and for strong fields ($\Omega_0,\Omega_2\gg\Omega_m$),

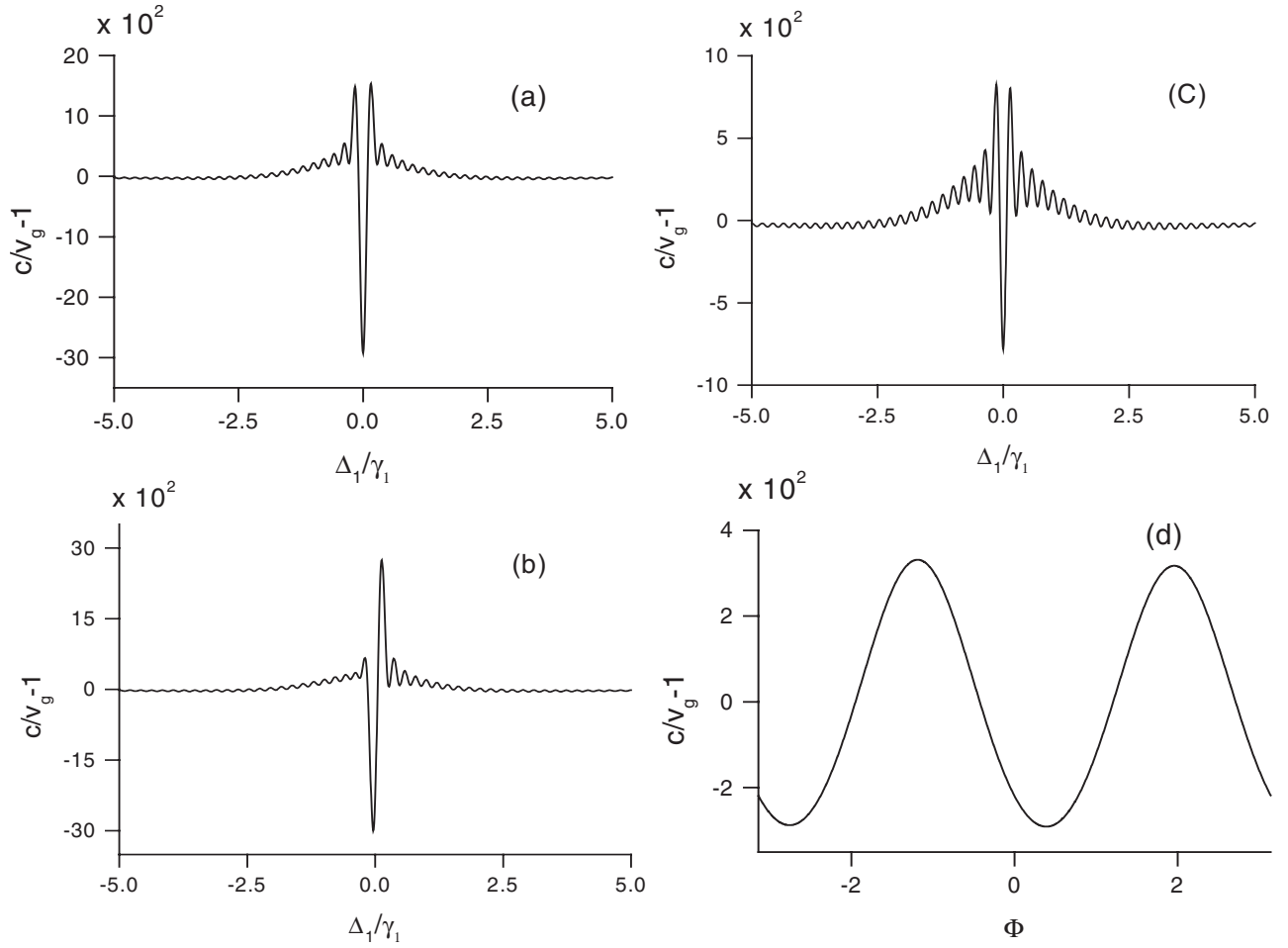

FIG. 5. Group index c/v_g-1 as a function of Δ_1/γ_1 in plots (a)–(c) and as a function of Φ in plot (d). The other parameters are $\Delta_0/\gamma_1=\Delta_2/\gamma_1=\Delta_m/\gamma_1=0$, $\gamma_1=\gamma_2=\gamma_3=1.0$, $\gamma_0=0$, $\Omega_1/\gamma_1=0.005$, $\Omega_0/\gamma_1=0.5$, $\Omega_2/\gamma_1=0.2$, and $\Omega_m/\gamma_1=0.5$. Plots (a), (b), and (c) are for $\Phi=0$, $\pi/3$, and $-\pi/4$, respectively. For plot (d) we keep $\Delta_1/\gamma_1=0$.

$$n_g(0)=\bar{n}+\bar{n}\Omega_{PL}^2\frac{\gamma_3^2\Omega_0^2+\gamma_0^2\Omega_2^2}{(\gamma_3\Omega_0^2+\gamma_0^2\Omega_2^2)^2}, \tag{8}$$

which decides the value of T_{abs} and hence the number of stored bits in this system.

IV. CONCLUSIONS

We have studied the phenomenon of EIT, its dispersion properties, and group-velocity variation in a four-level system having inverted-Y configuration in an asymmetric double quantum well system. Such a system can be considered to be composed of two three-level subsystems in Λ-type and ladder-type configurations. The EIT characteristics of both subsystems get combined in this four-level system as the coherences generated by the coupling field and the pumping field do not mutually destroy each other. By manipulating the system parameters and relative phases of the imposed fields it is possible to control the EIT characteristics of the system from a double-EIT to a single-EIT situation as well as from an absorption diplike EIT feature to dispersionlike EIT feature (situated at $\Delta_1/\gamma_1=0$) in both real and imaginary parts of the susceptibilities. Also, we can suppress the EIT due to one of the subsystems as desired by changing parameters including phase. Thus the results are nontrivial in comparison to any three-level EIT system. The striking impact is controllability of the group velocity and EIT bandwidth more effectively with greater flexibility and easiness in comparison to any three-level system. The consequences are the versatility and simplicity of such a system in practical applications. This kind of system is certainly useful in designing fast optical switching devices, which are based on the phenomenon of EIT as the variation of EIT and corresponding dispersion features are the main controllability parameters of such devices. The four-level system discussed here has been easily realized in a recent experiment.[8,17,18] Also, dispersion control by the single parameter of phase can find important applications in manipulating group velocity of light pulses and optical beam shaping.

ACKNOWLEDGMENTS

We acknowledge support from the University of Arkansas and Eastern Illinois University. The author is thankful to M. Xiao and S. Singh for helpful discussions.

*ajoshi@eiu.edu

[1] S. E. Harris, Phys. Today **50** (7), 36 (1997).
[2] M. Fleischhauer, A. Imamoglu, and J. P. Marangos, Rev. Mod. Phys. **77**, 633 (2005).
[3] J. Mompart and R. Corbalán, J. Opt. B: Quantum Semiclassical Opt. **2**, R7 (2000).
[4] A. Joshi and M. Xiao, in *Progress in Optics*, edited by E. Wolf (North Holland, Amsterdam, 2006), Vol. 49, p. 97 (and references therein).
[5] C. Ottaviani, D. Vitali, M. Artoni, F. Cataliotti, and P. Tombesi, Phys. Rev. Lett. **90**, 197902 (2003).
[6] H. Schmidt and A. Imamoglu, Opt. Lett. **21**, 1936 (1996); S. E. Harris and Y. Yamamoto, Phys. Rev. Lett. **81**, 3611 (1998); A. Joshi and M. Xiao, Phys. Lett. A **317**, 370 (2003).
[7] B. S. Ham and P. R. Hemmer, Phys. Rev. Lett. **84**, 4080 (2000); M. Yan, E. G. Rickey, and Y. Zhu, Phys. Rev. A **64**, 013412 (2001).
[8] S. M. Sadeghi, S. R. Leffler, and J. Meyer, Phys. Rev. B **59**, 15388 (1999); G. B. Serapiglia, E. Paspalakis, C. Sirtori, K. L. Vodopyanov, and C. C. Phillips, Phys. Rev. Lett. **84**, 1019 (2000); L. Silvestri, F. Bassani, G. Czajkowski, and B. Davoudi, Eur. Phys. J. B **27**, 89 (2002).
[9] H. Schmidt and A. Imamoglu, Opt. Commun. **131**, 333 (1996); S. Kocinac, Z. Ikonic, and V. Milanovic, IEEE J. Quantum Electron. **37**, 873 (2001); S. M. Sadeghi, H. M. van Driel, and J. M. Fraser, Phys. Rev. B **62**, 15386 (2000).
[10] M. D. Frogley, J. F. Dynes, M. Beck, J. Faist, and C. C. Phillips, Nature Mater. **5**, 175 (2006).
[11] M. E. Donovan, A. Shulzgen, J. Lee, P. A. Blanche, N. Peyghambarian, G. Khitrova, H. M. Gibbs, I. Rumyantsev, N. H. Kwong, R. Takayama, Z. S. Yang, and R. Binder, Phys. Rev. Lett. **87**, 237402 (2001).
[12] A. Joshi and M. Xiao, Appl. Phys. B: Lasers Opt. **79**, 65 (2004).
[13] M. Shapiro and P. Brumer, Rep. Prog. Phys. **66**, 859 (2003).
[14] E. A. Korsunsky, N. Leinfellner, A. Huss, S. Baluschev, and L. Windholz, Phys. Rev. A **59**, 2302 (1999); Y. Xue, G. Wang, J.-H. Wu, W.-H. Xu, H.-H. Wang, J.-Y. Gao, and S. A. Babin, Phys. Lett. A **324**, 388 (2004).
[15] P. Kral, I. Thanopulos, M. Shapiro, and D. Cohen, Phys. Rev. Lett. **90**, 033001 (2003).
[16] M. A. G. Martinez, P. R. Herczfeld, C. Samuels, L. M. Narducci, and C. H. Keitel, Phys. Rev. A **55**, 4483 (1997).
[17] J. F. Dynes, M. D. Frogley, J. Rodger, and C. C. Phillips, Phys. Rev. B **72**, 085323 (2005).
[18] H. Schmidt, K. L. Chapman, A. C. Gossard, and A. Imamoglu, Appl. Phys. Lett. **70**, 3455 (1997).
[19] S. Tsujino, A. Borak, E. Müller, M. Scheinert, C. V. Falub, H. Sigg, M. Giovannini, J. Faist, and D. Grützmacher, Appl. Phys. Lett. **86**, 062113 (2005).
[20] X. Hao, W.-X. Yang, X. Lu, J. Liu, P. Huang, C. Ding, and X. Yang, Phys. Lett. A **372**, 7081 (2008).
[21] J. B. Khurgin, J. Opt. Soc. Am. B **22**, 1062 (2005).